2026 IEEE International Conference on Robotics and Automation (ICRA 2026)
June 1-5, 2026. Vienna, Austria

Bioinspired Origami Exosuit for Sequential Lifting Assistance With Energy-Aware Compliance and Event-Triggered Impedance

Qunting Yang[1], Xiaoyu Wu[2], Bingcong Jian[2], Haisheng Xia[2] and Zhijun Li[2], *Fellow, IEEE*

***Abstract*— Back injuries resulting from manual material handling have long constituted a prominent threat to occupational safety. While back-support exosuits offer the potential to augment human strength, their practical implementation is hindered by persistent challenges pertaining to comfort and safety. Drawing inspiration from human biomechanics and muscle behavior, we develop a lightweight assistive exosuit that synchronizes with natural load-handling rhythms. By integrating a deployable Kresling origami structure with a two-stage transmission mechanism, a single motor can sequentially assist both the waist and arms, achieving motion-conforming support with minimal complexity. An energy-aware compliance control strategy allows the system to yield passively during unassisted motion, avoiding interference with voluntary human behavior. We propose an event-triggered impedance control strategy based on an energy tank framework, which adaptively intervenes only when interaction energy exceeds safety thresholds. Experimental results demonstrate substantial reductions in muscle activation during load-handling tasks, with decreases of up to 22.8%, 15.4%, and 14.8% in the biceps, triceps, and erector spinae ($MVC\%$), respectively.**

I. INTRODUCTION

Wearable robots, designed to be worn by users, assist in rehabilitation or enhance physical performance, making them ideal for interactive applications [1], [2], [3].

To mitigate the risks associated with manual handling of loads, researchers have increasingly explored robotic technologies to develop assistive systems aimed at reducing the physical strain on workers. In [4], the authors developed a wearable back robot for workers, using a series-elastic clutch actuator to assist hip motion and heavy load handling. In [5], the authors presented a passive spinal exosuit that incorporates carbon fiber beams and clutch-integrated springs. This design demonstrated significant reductions in both metabolic cost and muscle activity during lifting tasks. In [6], a spine-inspired continuum robotic joint was developed for soft exosuits, enabling improved alignment between robotic and biological joints for better conformal adaptation. Despite technological progress, existing exosuits still face limitations in supporting multiple degrees of freedom, as they are generally designed with one actuator assisting one body region—thus requiring multiple actuators to assist different body parts and thereby increasing weight and complexity. Therefore, a novel design should be explored to enable assistance for multiple body regions during manual handling tasks without imposing additional mechanical or metabolic burden on the user.

Origami, the ancient art of paper folding [7], has inspired numerous innovations in soft robotics. Its unique foldability enables the creation of deployable structures, leading to a variety of origami-based robots [8], including those capable of walking [9], variable wheel robots [10], manipulation [11], and crawling robots [12]. However, origami-based assistive devices for load handling have seen limited practical deployment to date. Building on the above-mentioned research, in this work, we propose a novel two-stage assistive mechanism based on the Kresling origami structure. This mechanism addresses the limitation of conventional assistive systems, which typically support only a single degree of freedom per actuator. This single motor sequentially drives the first-stage origami structure, converting rotational motion into linear displacement to assist the lower back. Once the motor torque exceeds the threshold of the stage transition layer, the second-stage origami is engaged, enabling additional assistance for arms. This design allows sequential actuation of both stages using a single motor, enhancing efficiency and reducing system complexity.

One widely used strategy for human-robot interaction is impedance control, which regulates the relationship between contact force and position via a virtual mass-spring-damper model. Since the foundational theories of impedance control were established, research has expanded into several key areas, including coupled stability analysis [13], force-tracking impedance control [14], and adaptive impedance control [15], etc. Building on these studies, we develop an impedance control framework incorporating a dual event-triggered mechanism. Unlike conventional approaches, our method initiates control actions based on both energy and power thresholds, adaptively modulating stiffness and damping to ensure safe and responsive interaction with external environments. Furthermore, when the user bends forward to lower a load, we introduce an energy-based detection strategy to identify active environments. This enables the assistive device to exhibit elasto-plastic compliance, allowing the origami structure to conform to user motion and emulate a leader-follower coordination pattern commonly observed in human teamwork.

In this paper, a novel soft wearable robot with a Kresling-origami-based two-stage transmission is presented, enabling sequential assistance to the lower back and arms using a

[1]Q. Yang is with the Department of Automation, University of Science and Technology of China, Hefei 230026, China, and also with Shanghai Key Laboratory of Wearable Robotics and Human-Machine Interaction, Shanghai 201804, China qunting@mail.ustc.edu.cn

[2]X. Wu, B. Jian, H. Xia and Z. Li are with the School of Mechanical Engineering, Tongji University, Shanghai 201804, China, and also with Shanghai Key Laboratory of Wearable Robotics and Human-Machine Interaction, Shanghai 201804, China wuxiaoyu@tongji.edu.cn; bingcongjian@tongji.edu.cn; hsxia@ieee.org; zjli@ieee.org (Corresponding author: X. Wu).

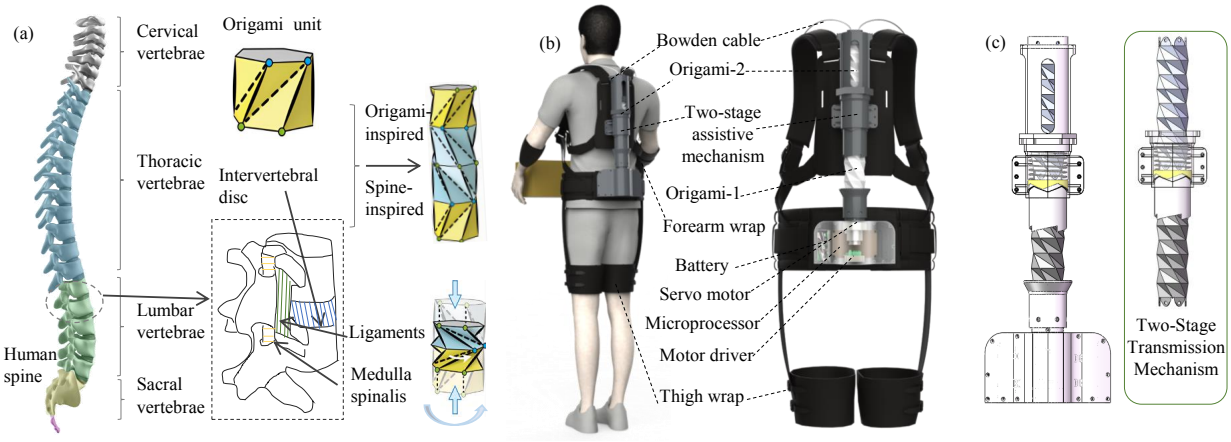

Fig. 1. **Bioinspired origami exosuit system.** (**a**) Design of the bioinspired origami mechanism. (**b**) The developed back-support exosuit. (**c**) Schematic of the two-stage transmission mechanism and electronic modules of the system.

single motor. The system integrates a dual event-triggered impedance controller with an energy-based compliance scheme to ensure safe and adaptive human-robot interaction. The main contributions of this work are summarized as follows:

- We propose a bioinspired time-sharing assistance mechanism that mimics the sequential force generation of human load handling-activating the waist before the arms. This design transforms a single motor's rotation into sequential longitudinal actuation through a deployable Kresling origami structure and a two-stage transmission.
- Based on a single-degree-of-freedom wearable origami system, we propose a novel event-triggered impedance control strategy grounded in an energy tank framework, with particular emphasis on human–robot coupled interaction during load-handling tasks.
- We develop an energy-aware adaptive compliance strategy that enables the exosuit to follow the user's motion during load-lowering.

II. SYSTEMS DESCRIPTION

A. Biomechanics-Inspired Exosuit Design

The human spine, composed of a series of vertebrae and intervertebral discs, supports body weight, protects the spinal cord, and enables flexion/extension, lateral bending, and axial rotation. The intervertebral discs, consisting of a collagen-rich annulus fibrosus and a gelatinous nucleus pulposus, act as fibrocartilaginous joints that withstand loads, absorb shocks, and allow limited motion between adjacent vertebrae.

The contraction and extension of the Kresling origami structure can effectively replicate the motion mechanism of the human spine. As illustrated in Fig. 1 (a), the origami unit mimics both vertebrae and intervertebral discs, offering a lightweight, symmetric structure suitable for wearable assistance. Furthermore, inspired by the sequential force generation observed in human load handling—where the waist engages prior to the arms—we propose a novel bioinspired time-sharing assistance exosuit that transforms the rotational input of a single motor into sequential longitudinal actuation via a deployable Kresling origami structure and a two-stage transmission system, as shown in Fig. 1 (b).

Specifically, the motor's rotary output induces origami-1 to rotate and collapse simultaneously, generating linear displacement that provides waist support forces. When the resultant contraction torque reaches the set threshold, the secondary transmission stage engages through a ratchet mechanism. This transfers torque to the origami-2, whose subsequent collapse delivers arm assistance via cable-driven linkage, maintaining synchronous multi-joint actuation while preserving single-motor efficiency. Unlike previous wearable exosuits that rely on multiple actuators, complex linkages, or compromise user comfort, this mechanism integrates an origami structure with coordinated dual-joint assistance, offering lightweight construction, reduced mechanical complexity, and synchronized support aligned with the natural rhythm of human motion. Compared with representative state-of-the-art back-support exosuits reported in [16], [17], [19], whose device weights are approximately twice ours (around 5.0-6.0 kg), our exosuit weighs only 2.5 kg, effectively reducing wearer burden by about 50%.

B. Two-stage Assistive Mechanism

The two-stage assistive mechanism distributes the driving force generated by the single-motor to the targeted assistive regions in a time-sequenced manner, as shown in Fig. 1 (c). The core of the mechanism is a compact stage-transition layer that regulates sequential torque distribution while maintaining the benefits of underactuation. It consists of a spring and a 3D-printed ABS housing. The spring within the stage-transition layer fixture acts as a clutch, preventing the stage transition layer from rotating initially, and then allowing it to rotate once the spring is compressed toward the thrust bearing at the top of the fixture. Specifically, when the motor drives origami-1 to contract, it provides assistance to the lumbar region while generating a rotational force. Once this rotational force reaches the threshold value, origami-2 is allowed to initiate rotation and thereby assist the upper limbs.

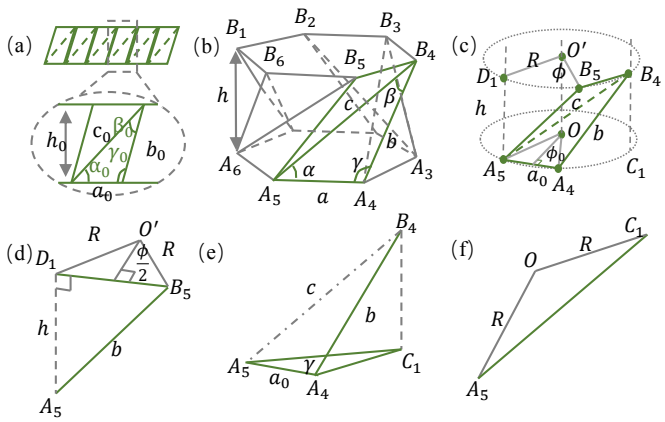

Fig. 2. **Basic kresling origami structure. (a)** Two-dimensional crease pattern of the Kresling origami with geometric parameters. **(b)** Three-dimensional folded module and its geometric definitions. **(c)** Panel $A_4A_5B_4B_5$ of the Kresling module at an arbitrary folding state. **(d)-(f)** Detailed views of three key segments of the Kresling structure.

C. Kresling Origami

The Kresling origami is defined by its 2D crease pattern (Fig. 2 (a)) and the resulting 3D module (Fig. 2 (b)). It consists of regular m-gons ($m = 6$ in Fig. 2), $2m$ triangular panels, and is parameterized by base length a_0, height h_0, and angle γ_0. The module geometry is described by height h, base radius R, and twist angle ϕ. As shown in Fig. 2 (c), the rotation angle ϕ is defined as the angle between the vectors $O'D_1$ and $O'B_5$, and the circumscribed circle radius R relates to the polygon side length a_0 as:

$$R = \frac{a_0}{2\sin\phi_0}, \tag{1}$$

where $\phi_0 = \frac{\pi}{m}$. With reference to the triangles $O'B_5D_1$ and $A_5D_1B_5$ shown in Fig. 2 (d), the lengths of the sides D_1B_5 and h can be obtained as follows:

$$|D_1B_5| = 2R\sin\frac{\phi}{2}, \tag{2}$$

$$h = \sqrt{b^2 - 4R^2\sin^2\frac{\phi}{2}}. \tag{3}$$

We define $\phi = \theta_a + \theta$, $\Delta h = h_a - h$, where θ_a and h_a denote the initial deflection angle and height of the single-layer origami structure, respectively. θ represents the rotation angle, and Δh represents the height variation corresponding to a rotation of angle θ. For origami structures that comprise $n(n \geq 1)$ layers, the following relation holds: $\Delta h_n = h_a - \sqrt{b^2 - 4R^2\sin^2\frac{(\theta_a+\theta-(n-1)\theta_b)}{2}}((n-1)\theta_b \leq \theta \leq n\theta_b)$. Then, we define $\Delta X = \Delta h_1 + \Delta h_2 + \cdots + \Delta h_n$ and $X = X_a - \Delta X$, where X denotes the instantaneous height of the origami structure as a function of the rotation angle. In the current configuration, the origami structure consists of $n = 6$ layers. The initial height $X_a = nh_a$ and the angle θ_b are both known constants. Taking the time derivative on both sides yields:

$$\dot{X} = J(\theta)\dot{\theta}, \tag{4}$$

where $J(\theta) = \sum_{k=0}^{5} \frac{-R^2\sin(\theta_a+\theta-k\theta_b)}{\sqrt{b^2-4R^2\sin^2\frac{\theta_a+\theta-k\theta_b}{2}}}$ enables the conversion of motor angular velocity $\dot{\theta}$ into the axial contraction velocity $\dot{X}$, providing a foundation for precise sequential actuation and integration with the energy-aware impedance control framework.

III. CONTROL DESIGN

During the assistance phase, when the user lifts a heavy object, the assistive device generates an upward force supporting both the waist and arms. If this assistive force momentarily exceeds safe human-robot interaction thresholds, it may pose a potential risk of injury to the lower back or upper limbs. Further, during the lowering phase, the extension of the origami structures must be precisely synchronized with the user's motion to provide continuous, appropriate interactive support and preserve user comfort throughout the task. Therefore, to address the issues in both phases, we develop dedicated control strategies to ensure safety and comfort during human-robot interaction.

A. Impedance Control Based on Dual-event Triggering

We consider a simplified one-degree-of-freedom assistive system modeled as a point mass with position θ, which is required to be driven toward a desired position θ_d. A physically interpretable controller capable of achieving this objective can be constructed by connecting a virtual spring between the mass and the desired reference point. The energy function of the system is therefore defined as:

$$E_{\text{tot}} = E_k + E_p = \frac{1}{2}J\dot{\theta}^2 + \frac{1}{2}k\theta_e^2, \tag{5}$$

where J represents the moment of inertia, $\dot{\theta}$ is the velocity, $\theta_e = \theta_d - \theta$. k represents the stiffness coefficient. E_k and E_p denote the kinetic energy and the potential energy, respectively. The objective is to formulate an impedance control strategy that incorporates knowledge of the human body's energy tolerance to prevent injury. To address the human-robot coupled interaction requirements during load handling, this study builds upon our previous work [18] to develop an event-triggered control strategy for a single-degree-of-freedom wearable exoskeleton that integrates a Kresling origami structure. The controller limits energy exchange with the operator by adjusting the stiffness parameter k, ensuring the system energy remains below a predefined threshold E_{set}, with particular emphasis on human–robot coupled interaction in load-handling tasks. Let $E_0 \geq 0$ as the initial energy of the system, and $t_u = \inf\{t > 0, |E_{\text{tot}} - E_0| < E_{\text{set}}\}$, and t_v denote the first time instant after t_u at which $|E_{\text{tot}} - E_0|$ reaches or exceeds the safety energy threshold E_{set} , then:

$$t_{(u+i)} = \inf\left\{t > t_{(v+i-1)}, |E_{\text{tot}} - E_0| < E_{\text{set}}\right\}, \tag{6}$$

$$\bar{k} = k, \quad t \in [t_{(u+i)}, t_{(v+i)}), \tag{7}$$

$$t_{(v+i)} = \inf\left\{t > t_{(u+i)}, |E_{\text{tot}} - E_0| \geq E_{\text{set}}\right\}, \tag{8}$$

$$\bar{k} = (2E_{\text{set}} + 2E_0 - J\dot{\theta}^2)/(\theta_d - \theta)^2,$$
$$t \in [t_{(v+i)}, t_{(u+i+1)}), \tag{9}$$

with stiffness $\bar{k} > 0$, and $i \in \mathbf{N}^+$ indicating the cycle number.

Power-based triggering complements the energy mechanism by regulating the dissipative damping coefficient to maintain safe interaction. We define the initial control torque as $\tau_c = k(\theta_d - \theta) - b\dot{\theta}$, then the instantaneous power is given by:

$$P_{tot} = \left(k(\theta_d - \theta) - b\dot{\theta}\right)\dot{\theta}, \tag{10}$$

where b is the damping coefficient. Let $P_0 \geq 0$ denote the initial power. The first triggering moments are defined as $t_k = \inf\{t > 0, |P_{\text{tot}} - P_0| < P_{\text{set}}\}$ and t_l denote the first time instant after t_k at which $|P_{\text{tot}} - P_0|$ reaches or exceeds the safety power threshold P_{set}, the subsequent operation cycles follow:

$$t_{(k+j)} = \inf\left\{t > t_{(l+j-1)}, |P_{\text{tot}} - P_0| < P_{\text{set}}\right\}, \tag{11}$$

$$\bar{b} = b, \quad t \in [t_{(k+j)}, t_{(l+j)}), \tag{12}$$

$$t_{(l+j)} = \inf\left\{t > t_{(k+j)}, |P_{\text{tot}} - P_0| \geq P_{\text{set}}\right\}, \tag{13}$$

$$\bar{b} = (k(\theta_d - \theta)\dot{\theta} - P_{set} - P_0)/\dot{\theta}^2, \tag{14}$$

$$t \in [t_{(l+j)}, t_{(k+j+1)}), \tag{15}$$

where $\bar{b} > 0$ denotes the damping coefficient. Then, we design the safety and energy-aware impedance control with dual-event triggering mechanism as follows:

$$\bar{\tau}_c = \bar{k}(\theta_d - \theta) - \bar{b}\dot{\theta}. \tag{16}$$

B. Energy Tanks

We model the energy tank as a virtual spring with state Q and energy $H(Q) = \frac{1}{2}Q^2$. Within the port-Hamiltonian framework, the interaction between the tank and the system is regulated by a transmission ratio T, leading to:

$$\dot{Q} = TP/J, \tag{17}$$

$$\dot{P} = -TQ, \tag{18}$$

where $P = J\dot{\theta}$. The transmission ratio T switches based on the tank energy: If $H(Q) > \eta$, then $T = -\bar{\tau}_c/Q$; if $H(Q) \leq \eta$ and the tank is discharging energy, then $T = 0$. Energy flows bidirectionally between the tank and the system: positive power ($\bar{\tau}_c\dot{\theta} > 0$) draws energy from the tank to actuate motion, while negative power ($\bar{\tau}_c\dot{\theta} < 0$) returns energy to the tank. This ensures passivity and stability under limited energy conditions. The final control torque is $\bar{\tau}_c = -TQ$.

C. Energy-based Compliance Control

During the lowering phase, we propose an energy-based method to detect active environments, enabling elasto-plastic compliance so the structure follows the user and mimics a leader-follower strategy. Specifically, the first step involves analyzing the energy flow to determine whether the external force originates from an active environment,

$$P_{\text{env}} = -\tau_c\dot{\theta}, \tag{19}$$

where P_{env} represents the work done by the environment on the robot. When P_{env} is positive, $P_{\text{env}} > P_{\text{thr}}$ and $|\tau_c| > \tau_{\text{thr}}$, it indicates that energy is transferred from the environment to the robot, suggesting the presence of an active environment. Here, P_{thr} is defined as the threshold of power, and τ_{thr} is defined as the threshold of interaction force. Once identified as an active environment, the plastic behavior of the robot is triggered: Let $\varepsilon = 1$ when $P_{\text{env}} > P_{\text{thr}}$ and $|\tau_c| > \tau_{\text{thr}}$, and $\varepsilon = 0$ otherwise, where $\varepsilon \in \{0, 1\}$ is a binary trigger variable based on energy flow detection, indicating whether an active environment is present and plastic compliance should be activated. Subsequently, based on the value of ε, the reference pose is adjusted to enable avoidance rather than resisting the external force. Then, the specific adjustment method is as follows:

$$\theta_d'(t) = \theta_d(t_0) + T_u \sum_{\tau=t_0}^{t} \left(v_d^*(\tau) + \varepsilon v_d(\tau)\right), \tag{20}$$

where $\theta_d'(t)$ denotes the updated reference pose at time t, incorporating plastic compliance to adapt to active environmental interactions. $\theta_d(t_0)$ is the initial reference pose at the starting time t_0, serving as the integration baseline. T_u represents the sampling period of the discrete-time control system. $v_d^*(\tau)$ is the desired reference velocity at time τ, generated by the control input. $v_d(\tau)$ is the actual robot velocity at time τ, reflecting the robot's current motion state.

IV. EXPERIMENTS VERIFICATION

In this section, experiments are conducted to validate the proposed adaptation control using the assistive exosuit. Six subjects (170±5 cm, 60±4 kg) were recruited, and informed of experimental procedures and provided informed consent. Approval of all experiments was granted by the Ethics Committee of Shenzhen Institute of Advanced Technology, Chinese Academy of Sciences (No. YSB-2021-Y0905).

A. Validation Experiment of The Controller

1) Experimental method: The controller validation experiment focuses on bending and lifting motions while wearing the assistive device. The object-lifting process consists of five distinct stages: upright, bending, pretension, lifting, and finally returning to the upright posture. As illustrated by the blue line in Fig. 3 (h), these stages correspond to Control Stage = 0, 2, 0, 1, and 0, respectively. Two different controllers are employed during the lifting (Control Stage = 1) and bending (Control Stage = 2) phases: the former applies impedance control with dual-event triggering, whereas the latter adopts compliance control. The initial stiffness coefficient $k = 20.0$, the damping coefficient at $b = 0.8$, and the energy pool corresponding to the spring storage states was set as $Q_0 = 30$ and $H_0 = 450$. $E_{set} = 15$, $P_{set} = 10$, the threshold $P_{\text{thr}} = 1.3$, and $\tau_{\text{thr}} = 1.5$.

2) Results and discussion: The experimental results validate the effectiveness of the proposed control strategies in ensuring safe and adaptive physical human-robot interaction during manual handling tasks. The dual event-triggered impedance control limited the interaction energy and power within predefined thresholds (Fig. 3 (a) and (b)) by dynamically adjusting the stiffness and damping coefficients (Fig. 3

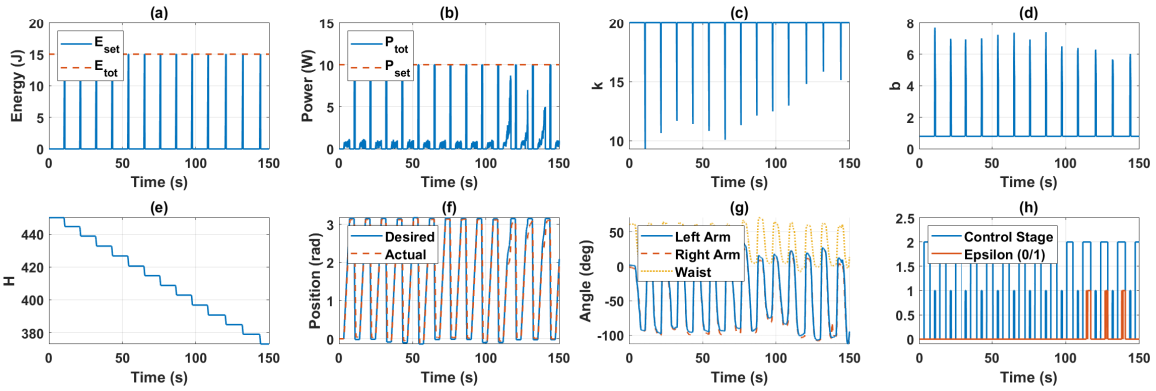

Fig. 3. **Experimental validation results of the controller across different control stages. (a)** Variation of total energy and set energy. **(b)** Variation of total power and set power. **(c)** Variation of stiffness coefficient. **(d)** Variation of damping coefficient. **(e)** Variation of total energy in the energy tank. **(f)** Position tracking of the motor. **(g)** Joint angle variations of waist and arms. **(h)** Control stages and Epsilon.

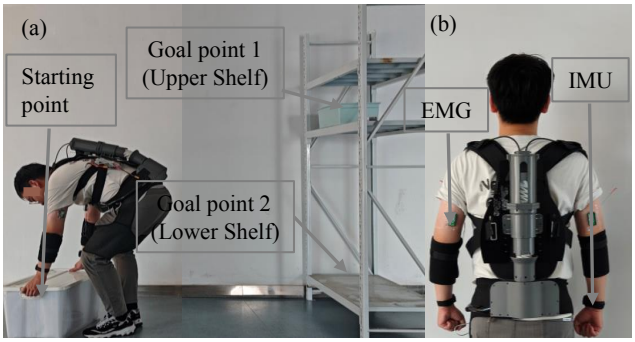

Fig. 4. **Experimental site and device setup**. **(a)** Lifting experiment area. **(b)** Subject equipped with the assistive device, IMUs, and EMG sensors.

(c) and (d)), ensuring safe loads on the user's waist and arms during lifting. The compliance control strategy demonstrated its efficacy in enabling natural motion synchronization during forward bending. When $\varepsilon = 1$ in the red regions of Fig. 3 (h), adjustments of the reference trajectory in Fig. 3 (f) were facilitated, conforming to the user's movement, thereby reducing resistance and enhancing comfort. This behavior emulates the leader-follower dynamics observed in human interactions, ensuring that the exosuit does not impede motion while still providing necessary support. The energy tank framework played a critical role in maintaining system passivity and stability. During the lifting phase, the energy tank's state in Fig. 3 (e) decreased as energy was expended to provide assistive torque, while remaining inactive during compliance control to avoid unnecessary energy dissipation. This approach ensures that the system operates within energy constraints, preventing instability due to excessive energy injection or depletion.

B. Validation Experiment for Assistive Exosuit Performance

To evaluate the performance of the proposed assistive exosuit, electromyography (EMG) sensors (United Kingdom, Biometrics, LE230) were used to monitor the changes in muscle activation along with inertial measurement units (IMU) sensors (China, WitMotion, BLC901CL) to assess the changes in the range of motion. Actuation was provided by a DC motor with an optical encoder (Switzerland, Maxon), and a drive unit (Israel, Elmo). Control of the motor and the data acquisition were performed by a microcontroller (China, LattePanda). The placement of the sensors is illustrated in Fig. 4 (b).

As shown in Figure 5, the task consists of four stages (a–d), with six experimental replicates performed at each stage. Data are presented as mean ± standard deviation (SD). The maximal voluntary contraction (%MVC) metric was used to validate the level of muscle activation and eliminate the variance in EMG signals caused by individual differences in muscle properties. The %MVC variations across the task are shown in the figure. For each target muscle, the mean and standard deviation of activation levels were computed and compared between the exosuit-assisted and unassisted conditions across all participants. Notably, during the task, biceps activation decreased by up to 22.8%, followed by triceps (up to 15.4%) and erector spinae (up to 14.8%). Paired t-tests confirmed that all reductions were statistically significant ($p < 0.05$). The reduction in arm muscle activation was more pronounced, as the erector spinae muscles not only lift the external load but also contribute to supporting the upper body mass. These results validate the exosuit's effectiveness in assisting users during complex lifting tasks.

V. Conclusion

In this paper, we present a Kresling origami-inspired soft wearable robot, driven by a single motor and featuring a two-stage transmission system that enables time-sequenced assistance to the lower back and arms during lifting tasks. Experimental results demonstrate substantial reductions in muscle activation during load-handling tasks, with decreases of up to 22.8%, 15.4%, and 14.8% in the biceps, triceps, and erector spinae ($MVC\%$), respectively, while avoiding potential injuries caused by excessive auxiliary force. Future research will focus on the optimal design of origami structures and adaptive control strategies in more complex task scenarios.

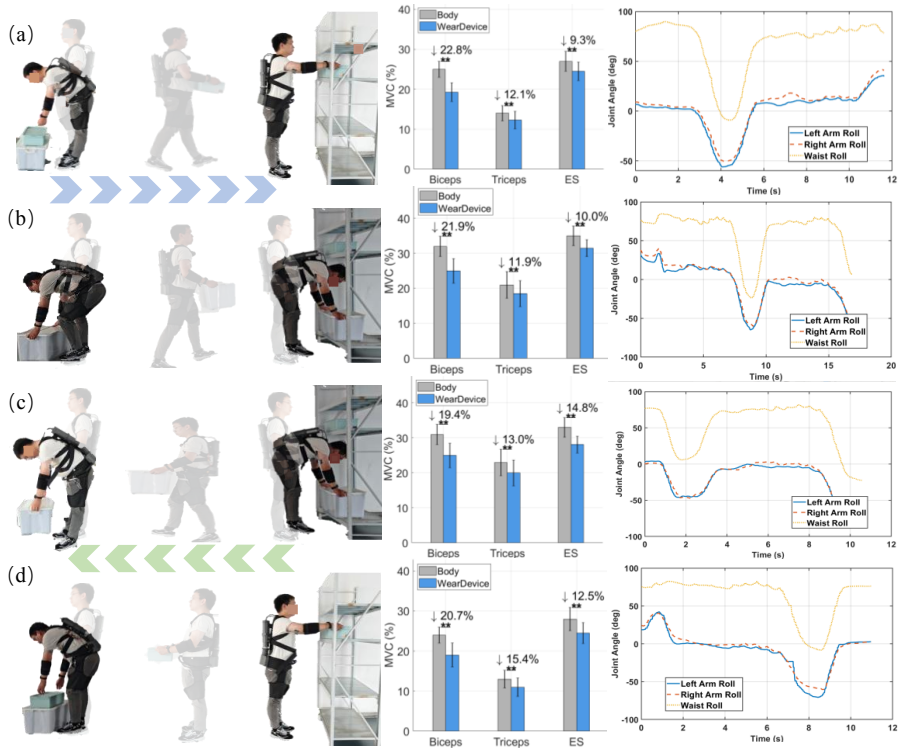

Fig. 5. **Experimental results of continuous multi-task load-handling. (a)** Transporting a small box from start to upper shelf. **(b)** Transporting a large box from start to lower shelf. **(c)** Returning large box from lower to start. **(d)** Returning small box from upper to start. Data are presented as mean ± SD, statistical significance is determined by paired t-test: $*p < 0.05$, $**p < 0.01$.

REFERENCES

[1] J. Kim *et al.*, "Reducing the metabolic rate of walking and running with a versatile, portable exosuit," *Science*, vol. 365, pp. 668–672, Aug. 2019.

[2] S. Toxiri *et al.*, "Back-support exoskeletons for occupational use: an overview of technological advances and trends," *IISE Transactions on Occupational Ergonomics and Human Factors*, vol. 7, no. 3–4, pp. 237–249, 2019.

[3] A. Prado, H. Zhang, and S. K. Agrawal, "Artificial neural networks to solve forward kinematics of a wearable parallel robot with semi-rigid links," in *Proceedings of the 2021 IEEE International Conference on Robotics and Automation (ICRA)*, Xi'an, China, May 2021, pp. 14524–14530.

[4] T. Zhang and H. Huang, "A lower-back robotic exoskeleton: industrial handling augmentation used to provide spinal support," *IEEE Robotics & Automation Magazine*, vol. 25, no. 2, pp. 95–106, Jun. 2018.

[5] M. M. Alemi, J. Geissinger, A. A. Simon, S. E. Chang, and A. T. Asbeck, "A passive exoskeleton reduces peak and mean EMG during symmetric and asymmetric lifting," *Journal of Electromyography and Kinesiology*, vol. 47, pp. 25–34, Aug. 2019.

[6] X. Yang *et al.*, "Spine-inspired continuum soft exoskeleton for stoop lifting assistance," *IEEE Robotics and Automation Letters*, vol. 4, no. 4, pp. 4547–4554, Oct. 2019.

[7] R. J. Lang, "The science of origami," *Physics World*, vol. 20, no. 2, p. 30, Feb. 2007.

[8] S. B. Arun and B. H. Anveeth, "Advancements in origami inspired robots, a review," in *Proceedings of the 2nd International Conference on Intelligent Computing, Instrumentation and Control Technologies (ICICICT)*, vol. 1, pp. 1293–1297, Jul. 2019.

[9] S. Miyashita *et al.*, "Robotic metamorphosis by origami exoskeletons," *Science Robotics*, vol. 2, no. 10, p. eaao4369, Sep. 2017.

[10] D. Y. Lee, G. P. Jung, M. K. Sin, *et al.*, "Deformable wheel robot based on origami structure," in *Proceedings of the IEEE International Conference on Robotics and Automation*, pp. 5612–5617, May 2013.

[11] S. Wu *et al.*, "Stretchable origami robotic arm with omnidirectional bending and twisting," *Proceedings of the National Academy of Sciences of the United States of America*, vol. 118, no. 38, p. e2110023118, Sep. 2021.

[12] H. Fang, Y. Zhang, and K. W. Wang, "Origami-based earthworm-like locomotion robots," *Bioinspiration & Biomimetics*, vol. 12, no. 6, p. 065003, Nov. 2017.

[13] H. Kazerooni, "Robust, non-linear impedance control for robot manipulators," in *Proceedings of the 1987 IEEE International Conference on Robotics and Automation*, Raleigh, NC, USA, Mar. 1987, pp. 741–750.

[14] T. Kim, S. Yoo, H. S. Kim, and J. Kim, "Design and force-tracking impedance control of a 2-DOF wall-cleaning manipulator using disturbance observer and sliding mode control," in *Proceedings of the 2018 IEEE International Conference on Robotics and Automation (ICRA)*, Brisbane, QLD, Australia, May 2018, pp. 4079–4084.

[15] Y. Zhang, D. Chen, A. E. P. Barceló, J. V. S. Luces, and Y. Hirata, "Adaptive incremental hybrid impedance control for robotic garment manipulation," in *Proceedings of the 2024 IEEE 20th International Conference on Automation Science and Engineering (CASE)*, Bari, Italy, Aug. 2024, pp. 2045–2051.

[16] J. Lee *et al.*, "Intelligent upper-limb exoskeleton integrated with soft bioelectronics and deep learning for intention-driven augmentation," *npj Flexible Electronics*, vol. 8, no. 1, p. 11, Feb. 2024.

[17] D. Lee, S. Lee, D. Lee, and D. Shin, "A soft wearable robot with an adjustable twisted string actuator and a two-stage transmission mechanism for manual handling tasks," *Advanced Intelligent Systems*, vol. 7, no. 5, p. 2400700, May 2025.

[18] Q. Yang, W. Ye, X. Wu, and Z. Li, "Safety and energy-aware impedance control of a continuum robot with vision-based manipulation," *IEEE Transactions on Automation Science and Engineering*, vol. , no. , pp. , 2025. doi: 10.1109/TASE.2025.3608039.

[19] H. Liao *et al.*, "Design, control, and validation of a novel cable-driven series elastic actuation system for a flexible and portable back-support exoskeleton," *IEEE Transactions on Robotics*, vol. 40, pp. 2769–2790, Aug. 2024.